Reconstructing historical atmospheric mercury deposition in Western Europe using: Misten peat bog cores, Belgium

Mohammed Allan [a,*], Gael Le Roux [b,c], Jeroen E. Sonke [d], Natalia Piotrowska [e], Maurice Streel [f], Nathalie Fagel [a]

[a] Argiles, Géochimie et Environnement sédimentaires, Département de Géologie, Université de Liège, Allée du 6 Août B18 Sart Tilman B4000-Liège, Belgium
[b] Université de Toulouse, INP, UPS, EcoLab (Laboratoire Ecologie Fonctionnelle et Environnement), ENSAT, Avenue de l'Agrobiopole, 31326 Castanet Tolosan, France
[c] CNRS, EcoLab, 31326 Castanet Tolosan, France
[d] Géosciences Environnement Toulouse, CNRS/IRD/Université de Toulouse 3, 14 avenue Edouard Belin, 31400 Toulouse, France
[e] Department of Radioisotopes, GADAM Centre of Excellence, Institute of Physics, Silesian University of Technology, Gliwice, Poland
[f] PPM, Département de Géologie, Université de Liège, Allée du 6 Août B18 Sart Tilman B4000-Liège, Belgium

HIGHLIGHTS

- Study of Hg concentration in four cores from Belgian peat bog.
- Reconstruction of Hg deposition over last 1500 years.
- Maximum Hg accumulation rates ranging from 90 to 200 μg $m^{-2}y^{-1}$ are recorded between 1930 and 1980 AD.
- The average Hg accumulation rate before the influence of human activities (e.g. 1300 AD) was 1.8 ± 1 μg $m^{-2}y^{-1}$.
- The predominant anthropogenic Hg sources were coal burning and smelter Hg emissions.

Keywords:
Atmospheric pollution
Coal combustion
Hg accumulation rate
Mercury
Multi-coring
Peat geochemistry

ABSTRACT

Four sediment cores were collected in 2008 from the Misten ombrotrophic peat bog in the Northern part of the Hautes Fagnes Plateau in Belgium. Total mercury (Hg) concentrations were analyzed to investigate the intra-site variability in atmospheric Hg deposition over the past 1500 years. Mercury concentrations in the four cores ranged from 16 to 1100 μg kg^{-1}, with the maxima between 840 and 1100 μg kg^{-1}. A chronological framework was established using radiometric ^{210}Pb and ^{14}C dating of two cores (M1 and M4). Pollen horizons from these two cores were correlated with data from two additional cores, providing a consistent dating framework between all the sites. There was good agreement between atmospheric Hg accumulation rates in the four cores over time based on precise age dating and pollen chronosequences. The average Hg accumulation rate before the influence of human activities (from 500 to 1300 AD) was 1.8 ± 1 μg $m^{-2}y^{-1}$ (2SD). Maximum Hg accumulation rates ranged from 90 to 200 μg $m^{-2}y^{-1}$ between 1930 and 1980 AD. During the European–North American Industrial Revolution, the mean Hg accumulation rate exceeded the pre-Industrial values by a factor of 63. Based on comparisons with historical records of anthropogenic activities in Europe and Belgium, the predominant regional anthropogenic sources of Hg during and after the Industrial Revolution were coal burning and smelter Hg emissions. Mercury accumulation rates and chronologies in the Misten cores were consistent with those reported for other European peat records.

1. Introduction

Mercury (Hg) has been used for thousands of years and more recently it has been used in a large number of industrial processes (Pacyna et al., 2006). Mercury is a metal that is toxic to humans and wildlife at low concentrations (Morel et al., 1998; Mergler et al., 2007). Natural Hg sources include volcanic activity, erosion and marine emissions (Schroeder and Munthe, 1998). The principal anthropogenic Hg emission sources are coal fired power plants, chlorine production, non-ferrous metallurgy, cement production, and primary and secondary lead and zinc production (Wilson et al., 2006; Pacyna et al., 2006; Pirrone and Mason, 2009). More than 95% of natural and anthropogenic Hg emissions are mainly in elementary form (Hg^0) with a residence time of 6–12 months in the atmosphere (Schroeder and Munthe, 1998; Fitzgerald and Lamborg, 2007; Pirrone and Mason, 2009). Long-range transport of Hg emissions has resulted in the contamination of remote ecosystems, generating a serious environmental problem that transcends national boundaries (Pirrone and Keating, 2010). Hylander and Meili (2003)

* Corresponding author. Tel.: +32 4 366 98 71; fax: +32 4 366 20 29.
E-mail address: mallan@doct.ulg.ac.be (M. Allan).

http://dx.doi.org/10.1016/j.scitotenv.2012.10.044

suggested that the current rate of global Hg emission (until 2000) to the atmosphere was approximately 3 times higher than during the pre-Industrial Revolution. The Industrial Revolution was a period from 1750 to 1850 marked by an increase in industrial activities, coal burning, and petroleum use. Similarly, Lindberg et al. (2007) estimated that atmospheric Hg deposition to remote ecosystems globally had increased by a factor of 3 since the start of the Industrial Revolution (1700 AD). To determine the regional versus global contributions, it is important to quantify the origin of this atmospheric Hg and its spatio-temporal variations.

Several types of environmental archives (lake and marine sediments, ice and peat) have been used to provide information about Hg deposition during the last thousand years (e.g., Gobeil et al., 1999; Bindler et al., 2001; Biester et al., 2002; Roos-Barraclough et al., 2002; Givelet et al., 2004a, 2004b). Peat records from ombrotrophic peatlands that receive inputs by way of the atmosphere are unique archives of anthropogenic and natural deposition of trace elements (e.g., Shotyk et al., 1996, 2001; Martinez Cortizas et al., 1997, Farmer et al., 2009; Zaccone et al., 2009; Manneville et al., 2006).

Data from ombrotrophic peat bogs, (Martinez Cortizas et al., 1999; Roos-Barraclough et al., 2002; Biester et al., 2002; Shotyk et al., 2003) have been utilized to reconstruct the evolution of atmospheric Hg deposition over long-term periods (e.g. the Holocene). In these studies, the Hg accumulation rate was calculated by combining the accumulation rate and density of the peat bog and Hg concentration (Madson, 1981; Jensen and Jensen, 1990; Norton et al., 1997; Martinez Cortizas et al., 1999; Roos-Barraclough et al., 2002; Givelet et al., 2004a, 2004b), and Hg was assumed to be immobile and well preserved in ombrotrophic peat (e.g. Benoit et al., 1998; Roos-Barraclough et al., 2002; Givelet et al., 2004a, 2004b; Shotyk et al., 2003, 2005). However, most authors (e.g. Rydberg et al., 2010; Biester et al., 2003) have suggested that Hg concentrations in peat bogs could be affected by natural biogeochemical processes such as peat decomposition and early diagenesis. This hypothesis was tested, but not validated, by Outridge et al. (2011) using an age-dated permafrost peat core from Northern Canada. Thus to use Hg concentrations in peat bogs as a record over time requires a precise chronological control of peat accumulation, especially in the acrotelm zone or the layer generally above the water table that can be both aerobic and anaerobic (Quinty and Rochefort, 2003). In this layer, unlike the catotelm or bottom layer that is below the water table, Hg should not be bound to recalcitrant and stable humic acids (Zaccone et al., 2009). Rydberg et al. (2010) further suggest that the local variability in Hg accumulation rates for different cores from the same bog may be explained by the variation in vegetation type in Swedish mire. In several studies a multi-core approach was used to reconstruct historical Hg accumulation in bogs (Benoit et al., 1998; Bindler et al., 1999, 2004; Klaminder et al., 2003; Novák et al., 2003; Coggins et al., 2006; Cloy et al., 2008; Martinez Cortizas et al., 2012; Zuna et al., 2012). By using 14 ombrotrophic peat cores collected from NW Spain, Martinez Cortizas et al. (2012) showed that the multi-core sampling provides good opportunities to evaluate the vertical, spatial and temporal records of atmospheric Hg deposition. To identify the different factors that influence mercury accumulation within and between sites we collected four cores in the Belgian Misten peat bog. The Misten peat has the two distinct layers (acrotelm/catotelm) controlled by the hydrological conditions. The microbial activity in the acrotelm is more rapid than in the catotelm. By coupling element chemistry with ^{14}C, ^{210}Pb dating, and pollen history, our aims were to: (1) quantify the net atmospheric Hg accumulation rates in the region of Misten (Belgium) over the last 1500 years; (2) determine the intra-site variability in Hg accumulation rate; (3) evaluate down core Hg mobility, and (4) compare the Misten record with Hg records from other European sites.

2. Materials and methods

2.1. Sampling site and sample collection

The Misten peat bog is located in Eastern Belgium, ~5 km from the German border (Fig. 1). The peat bog surface has higher relief than surrounding area. A titanium Wardenaar corer from the University of Heidelberg was used to recover the upper first meter. The length of all peat cores was between 90 and 110 cm. A Belarus corer was therefore used to core deeper (core name MIS-08-01b). Maximum peat thickness reaches up to 8 m (Wastiaux and Schumacker, 2003), dating back to 9000 years (De Vleeschouwer et al., 2007). Based on geochemical parameters (Ca/Mg ratio, Sr concentrations), the Misten peat bog described as ombrotrophic for the upper 6.5 m and minerotrophic between 6.5 and 8 m. Although, ombrotrophic peatlands receive inputs from the atmosphere, the minerotrophic component also receives water influenced by surrounding soils and rocks.

The four peat cores MIS-08-01W (M1), MIS-08-04W (M2), MIS-08-05W (M3) and MIS-08-06W (M4) were collected in February 2008 using a Wardenaar corer (Fig. 1) in the most protected part of the natural reserve "Les Hautes-Fagnes". The distance between the four cores was 50 to 100 m. The length of all peat cores was between 90 and 110 cm. Following the protocol described by Givelet et al. (2004a, 2004b), the cores were frozen (−40 °C) and cut by a stainless steel band saw (thickness of each sample ~1.5 cm). The peat samples were freeze-dried (at −40 °C, pressure ~ 10^{-1} mbar) during approximately 1 week and powdered using an agate ball mill.

2.2. Ash content and humification

The mineral matter content of the peat, defined as "ash content", was determined for all samples in cores M1 and M4 and every other sample in cores M2 and M3. Peat samples were dried at 105 °C over night and subsequently weighed to obtain the dry weight. Between 0.1 and 1 g of dried peat was then placed in oven at 550 °C for 6 h, to remove all organic matter by combustion (Chambers et al., 2011).

The degree of humification was estimated by colorimetry on peat alkaline extracts (Chambers et al., 2011). Two hundred milligrams of dried peat were reduced to powder and placed in an Erlenmeyer flask. One hundred milliliters of NaOH (8%) were added and the solution was boiled for 1 h. After cooling, the solution was diluted to 200 ml with MQ distilled water, then homogenized and filtered using no.1 Whatman filter paper. Fifty milliliters were taken and diluted with an equal volume of distilled water, and then directly placed in a spectrophotometer at the Scientific Station of the "Hautes Fagnes" (SSHF, University of Liege), for absorbance measurement at 540 nm. For every 10 samples, a standard with a humification level of 100% (Humic acid technical, ALDRICH) was included in the measurement. The ratio between the absorption values in the peat samples and peat standard was transformed to humification percentage.

2.3. Hg analysis

Mercury concentration was measured using a Milestone® DMA-80 at the Geosciences Environment Toulouse laboratory (France). All samples of the upper 25 cm of the cores and every other sample below this depth were measured. From 20 to 120 mg of dried bulk peat samples were used for analysis. Mercury concentrations were measured using an atomic absorption spectrophotometer after combustion and reduction of all forms of Hg to elemental Hg. Calibration was performed using ombrotrophic peat reference material (NIMT/UOE/FM/001/NIST 1575) and peach leaves (NIST 1547). During each series of analyses, standards were analyzed three times before the first sample then between the samples. The average measured values were $162 \pm 9 \mu g\ kg^{-1}$ ($n = 9$) for NIMT

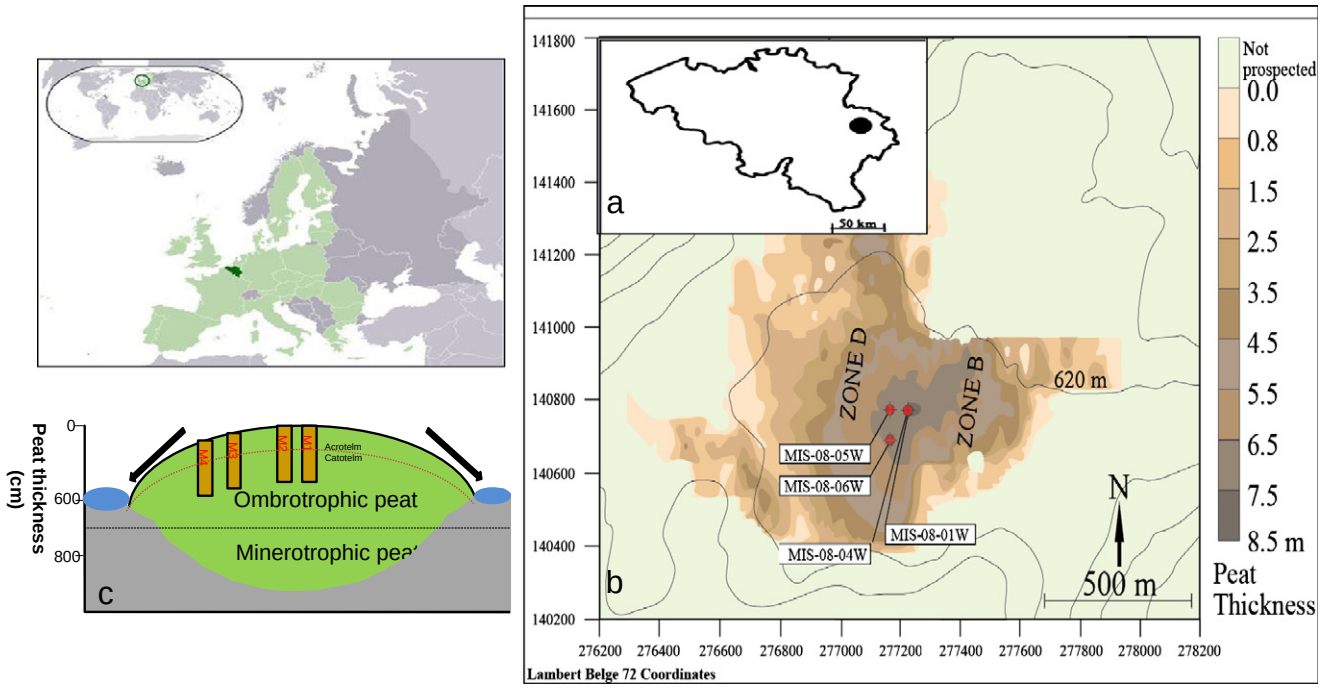

Fig. 1. (a) Smaller map shows location of Misten peat bog in Eastern Belgium, (b) map of the Misten peat bog modified from De Vleeschouwer et al. (2007), and (c) location of the coring sites. The color indicates the peat thickness as deduced from surface radar prospection (Wastiaux and Schoumakher, 2003). The red dots show the locations of the four peat bogs M1, M2, M3, and M4. (For interpretation of the references to color in this figure legend, the reader is referred to the web version of this article.)

(certified value 164 ± 20 μg kg^{-1}), 150 ± 30 μg kg^{-1} ($n = 5$) for NIST 1575 (certified value 150 ± 50 μg kg^{-1}), and 38 ± 3 μg.kg^{-1} ($n = 3$) for NIST 1547 (certified value 33 ± 5 μg kg^{-1}). All samples were analyzed in duplicate or triplicate.

2.4. Data analyses

Summary statistics were computed using Microsoft Office Excel 2010. The correlation coefficients (r) allow for the assessment of the degree of linear relationship between two variables. Relative standard deviation (% RSD) was calculated by divided mean Hg accumulation rates (Hg AR) by standard deviation (SD), which is expressed as %. Bulk density (g $cm-^{3}$) was estimated by dividing the dry weight (g) by fresh sample volume (cm^3). Hg AR (μg $m^{-2}y^{-1}$) were calculated as follows (Givelet et al., 2004a, 2004b):

$$\text{Hg AR} = 10 * [\text{Hg}] * \text{BD} * \text{PAR} \left(\text{cm y}^{-1}\right)$$

where [Hg] is the concentration (μg $kg-^{1}$), BD is the bulk density of the peat (g cm^{-3}), and PAR is the peat accumulation rate (cm yr^{-1}).

2.5. Elemental analysis

Fifty-five elements were measured in core M1 (unpublished data). Only lead (Pb), manganese (Mn), iron (Fe), calcium (Ca), magnesium (Mg), and titanium (Ti) are used in this study. Calcium and Mg are used to identify the peat status (ombrotrophic or minerotrophic peat, e.g. Shotyk et al., 1996). The concentrations of Ti is applied to quantify the natural "background" or lithogenic component of trace elements as brought by dust (Shotyk et al., 2001). Manganese and Fe are applied to understand the redox state of the samples (Steinmann and Shotyk, 1997). Lead is considered as immobile in the peat column and is largely enriched in the recent layers of European mires. It can be used as an indicator of the importance of the atmospheric input of anthropogenic trace metals.

Dry peat samples of ±100 mg were digested by microwave at the Institute of Earth Sciences (University of Heidelberg) using a mixture of HNO_3 (3 ml) and HBF_4 (0.1 ml). Organic matter was removed from the digested solution by addition of H_2O_2 (Krachler et al., 2002; Givelet et al., 2004a, 2004b). Element-concentrations were measured by inductively coupled plasma mass spectroscopy (Agilent quadrupole ICP-MS), at Geosciences Environment Toulouse laboratory (Toulouse, France). The plant standards (ICHTJ CTA-OTL-1 Oriental Tobacco Leaves, NIST tomato leaves 1573 and IAEA lichen 336) were analyzed with each series of samples, in order to determine the precision and reproducibility of analytical procedures. Comparison between reference values and measured values are satisfactory within 88–97%.

2.6. Age dating

Radiocarbon age dating was done using stems, branches or leaves of plant material collected under a binocular microscope. Samples were prepared at the GADAM Center for Excellence (University of Gliwice, Poland) and measured by acceleration mass spectrometer (AMS) in Poznan, according the protocol described by Piotrowska et al. (2010, 2011). Activities of ^{210}Pb were indirectly determined in cores M1 and M4 by the measurement of its decay product ^{210}Po using a Canberra 740 alpha spectrometer (Sikorski and Bluszcz, 2008; De Vleeschouwer et al., 2010). The constant rate of supply (CRS) model (Appleby, 2008) was applied for the ^{210}Pb dating. The maximum depth at which ^{210}Pb could be detected was 22 cm for the core M1 (Table 1). Ten samples in the core M1 were dated by this method (Table 2). The M1 (200 cm) was cross referenced using the Wardenaar section and two Belorussian sections from the Misten peat bog previously dated. In this study we focus on the upper Wardenaar core (M1).

The composite age-depth for M1 was obtained by coupling the ^{14}C and ^{210}Pb to generate an age interval for each sample (Piotrowska et al., 2010, 2011). The ^{210}Pb age was obtained by applying a Gaussian distribution of an age a function of depth, with a standard deviation of several years (Piotrowska et al., 2010). The total

Table 1
Results of ^{210}Pb measurements and CRS modeling for 01W core.

Core	Composite depth (cm)	CRS ^{210}Pb age AD	Uncertainty (years)
MIS-08-01W	1.1	2008	1
MIS-08-01W	3.0	2007	2
MIS-08-01W	4.3	2006	2
MIS-08-01W	5.2	2005	2
MIS-08-01W	6.1	2004	2
MIS-08-01W	7.0	2003	2
MIS-08-01W	7.9	2002	2
MIS-08-01W	8.8	2001	2
MIS-08-01W	9.7	2000	2
MIS-08-01W	10.6	1998	2
MIS-08-01W	11.5	1997	2
MIS-08-01W	12.4	1996	2
MIS-08-01W	13.3	1995	2
MIS-08-01W	14.2	1994	2
MIS-08-01W	15.1	1991	2
MIS-08-01W	16.0	1987	2
MIS-08-01W	16.9	1981	2
MIS-08-01W	17.8	1973	2
MIS-08-01W	18.7	1966	2
MIS-08-01W	19.6	1954	2
MIS-08-01W	20.5	1938	2
MIS-08-01W	21.4	1903	3
MIS-08-01W	22.3	1859	3

activity of ^{210}Pb (C_{tot}) was determined using the formula according to Appleby, 2001:

$$C_{tot} = C_{tot}(0)e^{-\lambda t} + C_{sup}\left(1-e^{-\lambda t}\right)$$

where C_{sup} is the supported activity, λ is the ^{210}Pb radioactive decay constant and C_{tot} (0) is the total ^{210}Pb activity of the sediment at the time of burial.

All ^{210}Pb and ^{14}C data were processed using the 'Bacon' software (Blaauw and Christen, 2011) to establish an age model and age range for each peat section (Fig. 2).

2.7. Pollen analysis

The obtained age-depth model for C1 and data from the a core previously described by De Vleeschouwer et al., 2012, were applied along with the pollen horizons to stratigraphically correlate the four cores. The pollen and spore composition for each of the four cores were analyzed at the Palaeobiogeology, Palaeobotany and Palaeopalynology laboratory (University of Liege, Belgium). About 2 g of fresh peat were treated with hydrochloric acid (HCl, 10%), pure acetic acid and acetolysis and the residues were washed by sieving through 200 μm and 12 μm meshes. The pollen and spore residues were suspended in glycerol, identified and counted at ×400 magnification using JENAVAL microscope. Pollen zones were determined by using the relative percentage of arboreal forest vegetation pollen and spores (AP) and non-arboreal pollens (NAP) types according to the procedure outlined by Vincens et al. (2007). Nine zones were defined in cores M1 and M4 (Table 3) that were correlated to those found in M2 and M3 (Fig. 3). First, the pollen zones were directly defined by comparing cores M1 and M4 (the best age-dated records). Second, the zonation was established for cores M2 and M3 which were not ^{210}Pb age-dated and only ^{14}C age dated at the bottom (Table 2). The upper sections of cores M2 and M3 were dated by combining pollen chronology, sedimentation rates, and ^{210}Pb and ^{14}C dates from the cores M1 and M4 (Table 2).

Table 2
Results of ^{14}C dating for cores 01W, 04W and 05W. Calibrated age ranges obtained with use of OxCal program (Bronk Ramsey, 2009) and IntCal09 calibration curve (Reimer et al., 2009).

Core	Composite depth (cm)	^{14}C age BP	Calibrated age range AD/BC* (95.4% probability interval)
MIS-08-01W	28.6	90 ± 30	1680–1930 AD
MIS-08-01W	38.6	590 ± 30	1300–1415 AD
MIS-08-01W	53.6	920 ± 35	1030–1210 AD
MIS-08-01W	69.9	1365 ± 35	610–770 AD
MIS-08-01W	90.8	1500 ± 30	440–640 AD
MIS-08-01b	112.7	1780 ± 30	135–340 AD
MIS-08-01b	135.5	2085 ± 30	190–40 BC
MIS-08-01b	153.2	2240 ± 35	390–205 BC
MIS-08-01b	175.9	2185 ± 35	380–170 BC
MIS-08-01b	205.5	2530 ± 35	800–540 BC
MIS-08-04W	108.7	1500 ± 30	440–639 AD
MIS-08-05W	93.2	1125 ± 30	783–991 AD

* BC stands for "before Christ" and AD stands for "after death."

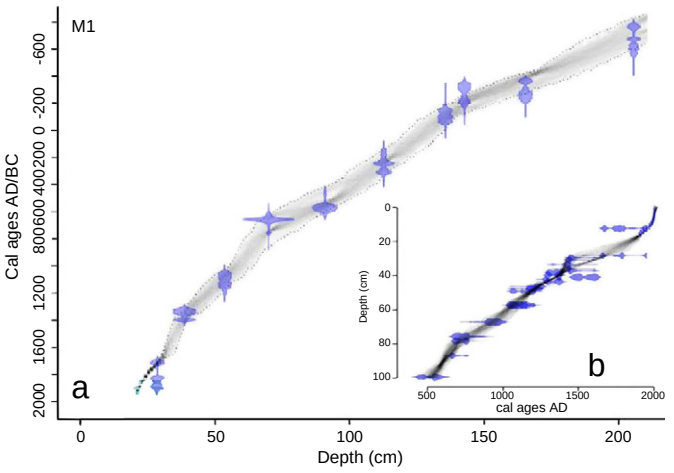

Fig. 2. Age-depth model for core M1 obtained by coupling 210 Pb with 14C (a), and (b) M4 age model (DeVleeschouwer et al., 2012). Gray-scales indicate all likely age-depth models, and dotted lines indicate the 95% confidence ranges. (For interpretation of the references to color in this figure legend, the reader is referred to the web version of this article.)

3. Results

3.1. Density, ash content and humification

In core M1 peat accumulation rate increased slightly from 100 cm at base to 2 mm yr^{-1} at 84 cm depth (447–692 AD) and then declined to 22 cm (1850–1864 AD) were it was lowest value (0.2 mm yr^{-1}). From this depth upward, the values increase again and reach a maximum of 15 mm yr^{-1} at the peat surface (2008–2011 AD). The peat accumulation rates were calculated for cores M2 and M3, considering that the accumulation rate is constant in all pollen zones, by using the correlation between pollen record and the age dating of cores M1 and M4.

Peat density in the 4 cores varied from 0.01 g cm^{-3} to 0.2 g cm^{-3}, reflecting the shift from the living plants of the bog acrotelm to the catotelm (Fig. 4). Thus density values increase from the lower part of the cores up to 15–25 cm, and then they decrease to the surface.

Ash contents of 0.3–10% are typical of ombrotrophic peats (Fig. 4). In the case of Misten bog, higher values around 10% can indicate additional input of inorganic particles by human activities: eroded soil particles but also industrial particles from coal burning and smelting. The degree of humification is very low (≤20%) in the upper 10–15 cm and generally increases with depth (Fig. 4).

3.2. Hg concentrations

Average Hg concentrations were similar in the lower part of the four cores (35 ± 15 μg kg^{-1}), and gradually decreased from ~30 to 40 cm to reach a maximum value between 13 and 27 cm (Fig. 4). The maximum Hg concentration recorded in core M1 was 840 μg kg^{-1} (at 19 cm-depth), core M2 was 890 μg kg^{-1} (at 27 cm-depth), core M3

Table 3
Comparison date, thickness and pollen zones for the Misten cores. Each pollinic zone has a different characters AP (arboreal pollen) and NAP (non-arboreal pollen).

Pollen zone	No	Age model for 01W AD	Age model for 06W AD	Main AP criteria	NAP criteria	Total AP %	Total NAP %
Xd4	9	2005–2008		*Picea* dominance	*Ericaceae* development	36	12
Xd3	8	2000–2004	2002–2007	*Picea*≫	*Ericaceae* development	84	12
Xd2	7	1996–1998	2000	*Picea*	*Ericaceae* development	75	18
Xd1	6	1965–1995	1969–1998	*Picea*>	*Ericaceae* development	71	26
Xc	5	1788–1953	1790–1946	*Quercus. Betula. Pinus. Picea*	*Plantago* maximum, *Poaceae* max (30%)	50	46
Xb	4	1566–1780	1431–1759	*Quercus*≫*Fagus*	*Cerealia* max (>10%)	55	41
Xa	3	1062–1520	1170–1425	*Fagus*≥*Quercus*	*Poaceae*<20% *Cerealia*<6%	66	28
IXe	2	684–1039	666–1153	*Fagus*≥50%	–	82	15
IXd	1	533–635	503–648	*Fagus*≥50%	*Cerealia* development	86	11

was 870 μg.kg^{-1} (at 18 cm-depth), and in core M4 was 1130 μg kg^{-1} (at 12 cm-depth). For the core M1, the concentrations average 35 ± 9 μg kg^{-1} from the base (91 cm) to 34 cm-depth. For the cores M2 and M3, Hg concentrations start to increase occurred at 35 and 25 cm deep, respectively. Below these depths the average concentrations is 46 ± 13 μg kg^{-1} (35 to 108 cm), and 45 ± 12 μg kg^{-1} (25 to 93 cm), respectively. For the core M4 the onset of the major Hg increase occurs at 29 cm-depth, below this depth average Hg concentration is 37 ± 10 μg kg^{-1}. In the upper most section of the four cores, Hg concentration decreased to values 45 μg kg^{-1} (0 cm-depth) for M1, 30 μg kg^{-1} (1.5 cm-depth) for M2, 29 μg kg^{-1} (1 cm-depth) for M3, and 70 μg kg^{-1} (1 cm-depth) for M4. Maximum humification values occurred in the lower sections, while the maximum Hg concentration was observed in the upper section of the catotelm (between 15 and 30 cm) for all the cores. In the Misten peat cores, correlation coefficients between mercury concentration and the humification were calculated. There was no significant correlation between Hg concentration and humification (for cores M1 and M4 $r = -0.11$, for core M2 $r = 0.3$ and for core M2 $r = 0.07$).

3.3. Pb, Ti, Mn, Fe, Ca, and Mg concentrations

Major elements, Pb and Ti were investigated for only core M1. Calcium and magnesium concentrations are relatively constant in

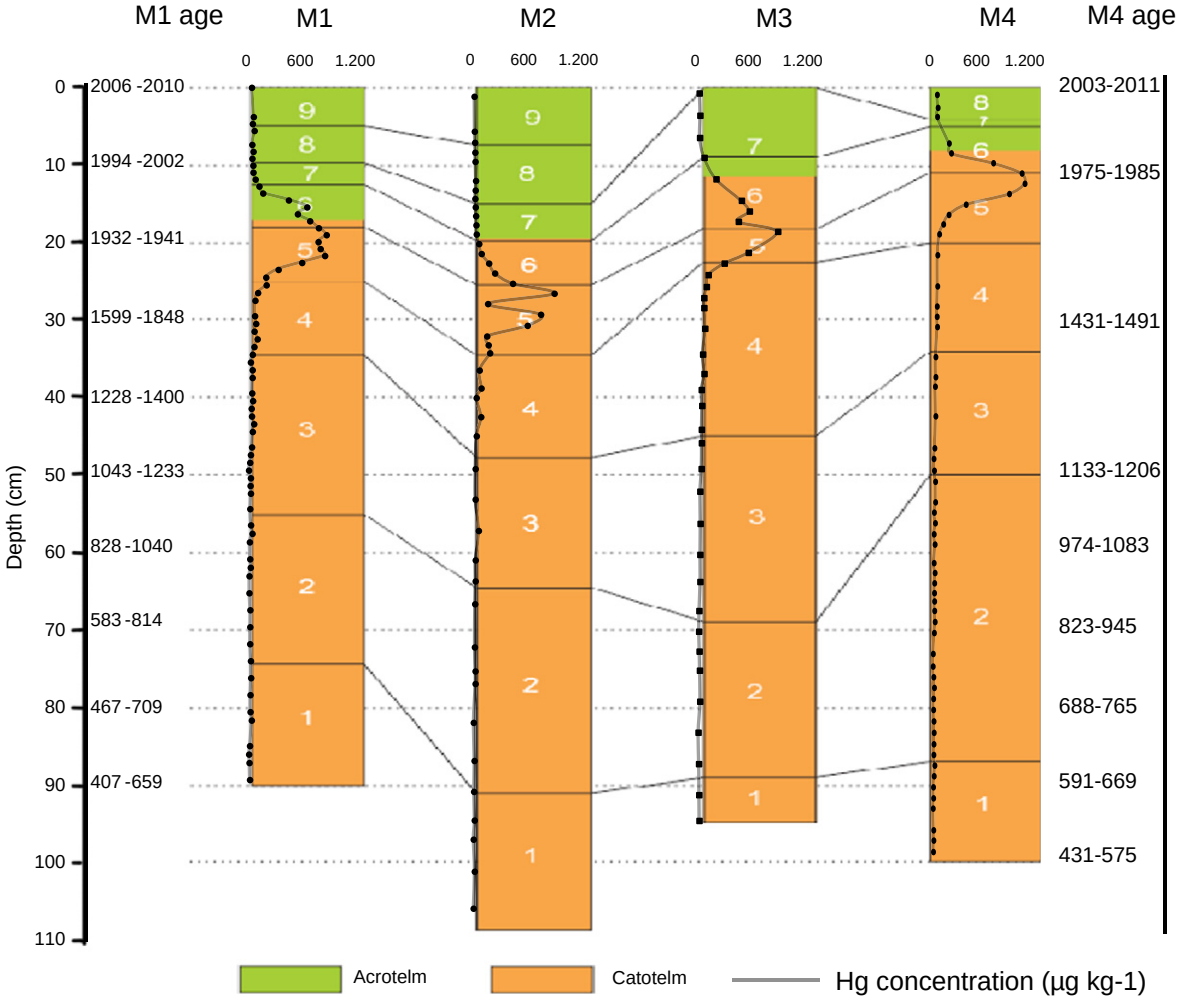

Fig. 3. The correlation of pollen zones in the four cores. The green color shows the acrotelm and the brown color is the catotelm. Black line is the concentration of Hg in the four cores.

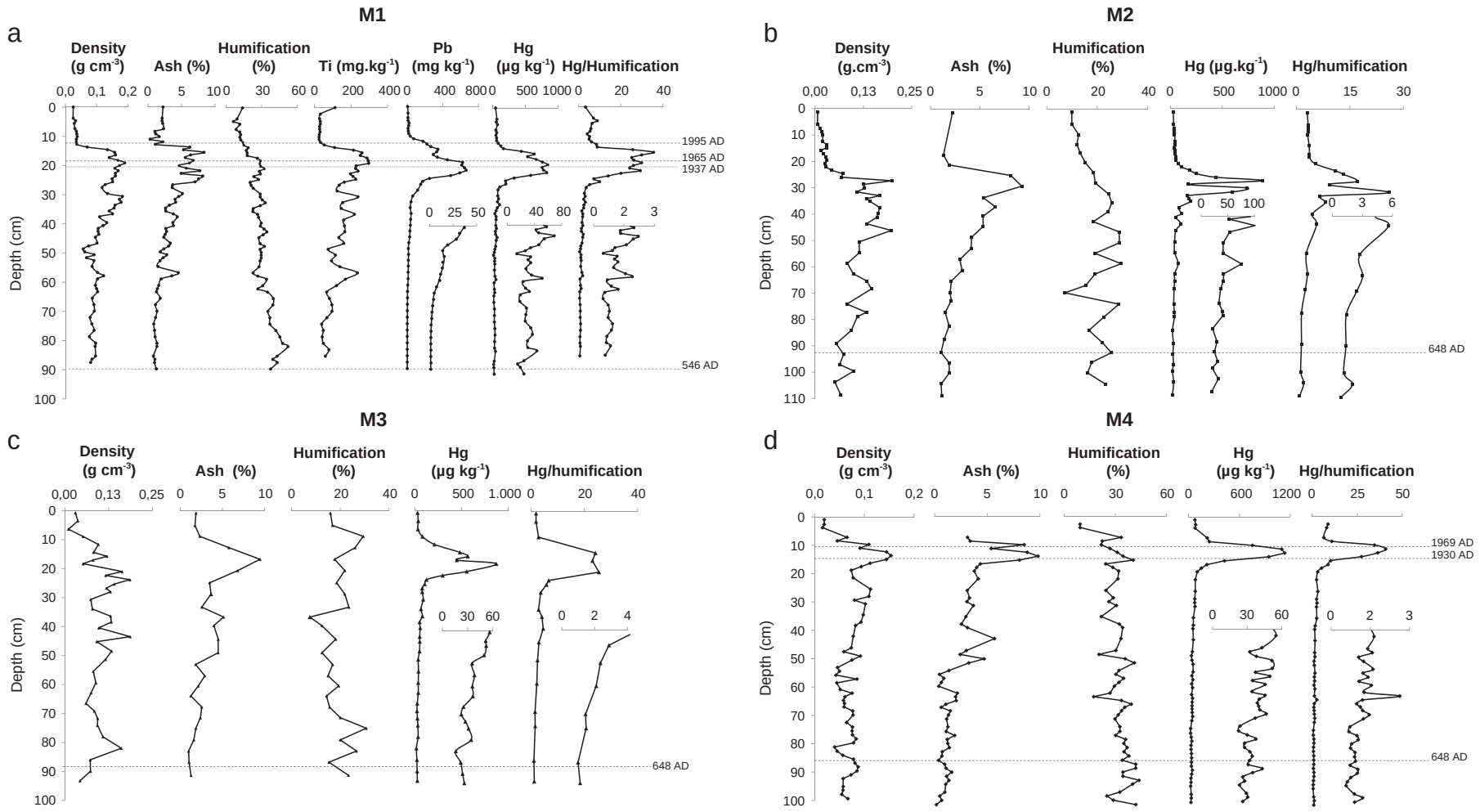

Fig. 4. Profiles of bulk density (g cm^{-3}), ash content (%), humification (%), Ti and Pb concentration (mg kg^{-1}), Hg concentration (µg kg^{-1}), ratio Hg/humification, and pollen zones versus depth. (a) core M1, (b) core M2, (c) core M3, and (d) core M4.

the catotelm layer. In the upper most section (catotelm layer) of this core, Ca and Mg concentrations increased to values > 2000 and 300 mg kg^{-1}, respectively. The Mg/Ca ratio ($\approx 0.23 \pm 0.11$) is similar the average rainwater in this area confirming that the Misten peat is ombrotrophic.

Titanium concentrations showed a large increase at catotelm–acrotelm boundary (Fig. 4a). Titanium concentrations were not correlated with Fe (correlation coefficients $r = 0.34$).

Iron is a major element susceptible to redox processes at the acrotelm–catotelm boundary (Gobeil et al., 1999) and Pb input may come from the surrounding watershed or from the atmosphere. Between 18 cm and the peat surface, the concentrations fall to 110 μg g^{-1} (Fig. 4a).

Lead values increase from the base of the core, and abruptly peak at 660 mg kg^{-1} within 5 cm under the acrotelm–catotelm boundary. They then decrease abruptly above this boundary but remained elevated at 400 mg kg^{-1}. Lead concentration decreases to 5 mg kg^{-1} in surface (Fig. 4a). Manganese and iron concentrations are almost constant in the lower sections of core M1 (3 ± 1, 330 ± 60 mg kg^{-1}, respectively). Manganese and iron concentrations increase in the upper sections, and decrease to the surface of the core M1 (Fig. 5).

3.4. Hg accumulation rates

In order to examine the historical record of Hg pollution over the last 1500 years, Hg accumulation rates, and Hg AR (μg $m^{-2}y^{-1}$) were calculated for the four cores studied (Fig. 6). Hg accumulation rates in M1 averaged ~2 μg $m^{-2}y^{-1}$ from 533 to 1611 AD. The mean values increase from 4 μg $m^{-2}y^{-1}$ at the start of the Industrial Revolution (1691 AD) to >170 μg $m^{-2}y^{-1}$ at 1953 AD. Mercury accumulation rates increased to 115 μg $m^{-2}y^{-1}$ (1965 AD), and decreased slightly to 111 μg $m^{-2}y^{-1}$ (1975 AD). Mercury accumulation rates increase to a maximum of 179 μg $m^{-2}y^{-1}$ (1987 AD), followed by a decreased to the surface of the core (20 μg $m^{-2}y^{-1}$, Fig. 6). In M2 and M3 cores, Hg accumulation rates remain constant at a mean value of 3 ± 1.4, 1.2 ± 0.4 μg $m^{-2}y^{-1}$ respectively, from the base of M2 and M3 cores to 50 cm of depth, and increase to maximum values of 88 and 193 μg $m^{-2}y^{-1}$, respectively. The Hg accumulation rates declined towards the top of the core to 5 and 38 μg $m^{-2}y^{-1}$, respectively. In the core M4, Hg accumulation rates remained constant at a mean value of 1.4 ± 0.8 μg $m^{-2}y^{-1}$ from 503 to 1603 AD. In the upper 25 cm of the core, Hg accumulation rates increased from 4 μg $m^{-2}y^{-1}$ (1664 AD) to a maximum ~120 μg $m^{-2}y^{-1}$ (1930 AD), followed by a decline to 8 μg $m^{-2}y^{-1}$ (2007 AD) at the surface (Fig. 6). There was a significant correlation between Hg AR in the four cores ($r \geq 0.87$).

4. Discussion

4.1. Effects of biogeochemical processes on Hg concentration

Previous work (e.g. Biester et al., 2003; Zaccone et al., 2009) suggested that Hg concentrations in peat bog cores may be affected by different biogeochemical processes (diagenetic processes, peat decomposition and humification). Similarly, Fe and Mn reactivity are influenced by similar processes (e.g. Steinmann and Shotyk, 1997). Some elements adsorbed on Fe and Mn hydroxides can be remobilized and redistributed during the redox processes (i.e. arsenic and phosphorus; Steinmann and Shotyk, 1997). In anoxic conditions, Fe and Mn oxides release Fe (II) and Mn (II) to the porewaters (Gobeil et al., 1999). These reduced forms will diffuse upward until they reach the oxic zone and become oxidized (Steinmann and Shotyk, 1997; Matty and Long, 1995). If Hg showed similar behavior then the maximum Hg concentration would be correlated with maximum in Fe and Mn concentrations in the upper layers of peat cores at catotelm–acrotelm interface.

In core M1, Fe and Mn concentrations were measured and compared with Hg concentration (Fig. 5). The maximum Hg concentrations in core M1, at 19 cm, are below the maximum Fe and Mn concentrations at 16–6 cm-depth. Normalizing Fe, Mn and Hg to a conservative element such as Ti showed that the maximum Hg/Ti ratio corresponded to the minimum in Fe/Ti and Mn/Ti ratios (Fig. 5). Such observation suggests that the Hg concentration profiles measured in the Misten bog were not affected by redox or diagenetic processes.

In a study on Patagonian cores, Biester et al. (2003, 2012) showed that Hg concentration is influenced by peat decomposition processes and mass losses, and suggested that Hg concentrations in peat do not solely reflect the variations in external Hg flux. However, Biester et al. (2012) recently showed using data collected from a peat bog in the Harz mountains, Germany, that "peat decomposition may have played only a minor role" in Hg distribution in the peat column illustrating the specificity of each site in preserving or not the Hg historical signal. The lack of correlation between humification and Hg concentrations also suggests that the peat decomposition is not playing a major role in Hg variability in Misten peat cores.

Others factors could also influence the Hg concentrations in peat. For instance, differences in the structure and morphology of the bog can indicate heterogeneous peat accumulation rates (Rydberg et al., 2010), as

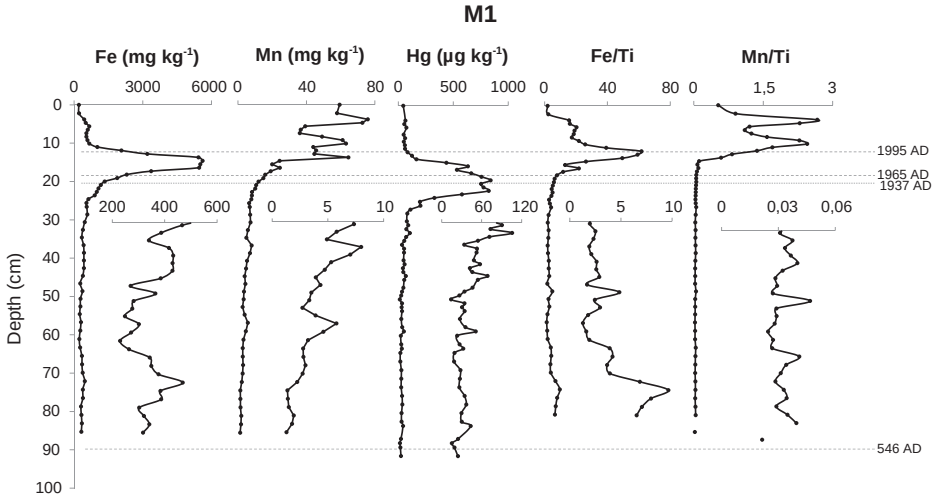

Fig. 5. Concentrations of Hg (μg kg^{-1}), Mn (mg kg^{-1}) and Fe (mg kg^{-1}), Fe/Ti and Mn/Ti ratio for the M1 core. Note that the maximum in Hg concentrations corresponds to minima in Fe/Ti in M1 core.

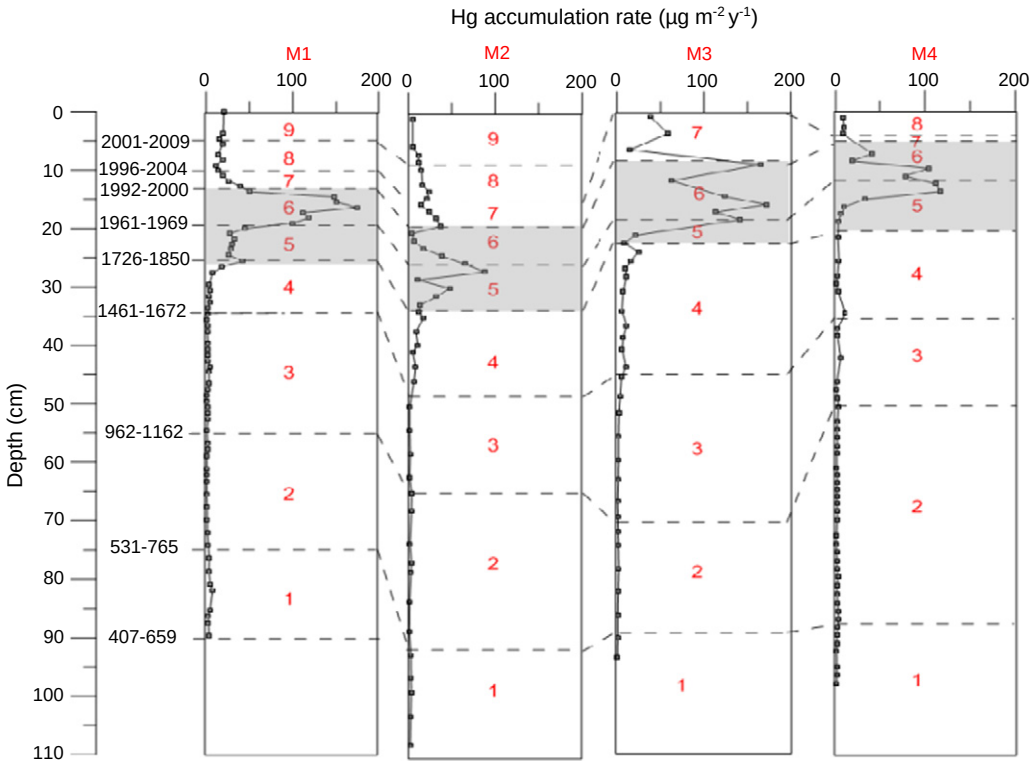

Fig. 6. Calculated total accumulation rate of Hg (AR) for the Misten peat bogs cores (M1, M2, M3, and M4). Gray zone: maximum accumulation rates of Hg, number 1–9: pollen zonation.

observed in the Misten bog (Figs. 1c, 3). Despite the fact that the four cores were sampled in the most raised part of the bog, there were differences in peat accumulation rates between the four cores suggesting a recent heterogeneous growth of peat (Figs. 1c, 3). Similarly the peak Hg concentrations in each core are not located at the same depths. For example, the maximum Hg concentration for M1 was at 19 cm, for M2 at 27 cm, for M3 at 18 cm and for M4 was at 12 cm. However the change in Hg concentrations was similar as a function of age (Fig. 4).

In summary, biogeochemical processes do not appear to have affected the Hg profiles in Misten peat cores. The maximum Hg concentrations occur between 12 and 27 cm-depth and the change in Hg concentrations are similar across time and pollen zones (Fig. 4). The similar chronologies of Hg records in the four peat cores suggest that the atmospheric Hg deposition is the main process affecting the Hg profiles. Several studies showed that Pb is an immobile element in ombrotrophic peat bogs (e.g. Shotyk et al., 1998; Le Roux et al., 2005). In core M1, the correlation between Hg and Pb concentration (correlation coefficients $r = 0.7$) showed similar chronology and distribution (Fig. 4a). The similarity between Hg and Pb profiles suggest that Hg is immobile as well in these cores.

4.2. Intra-site variability in Hg accumulation rates

Roos-Bacclarough and Shotyk (2003) compared both inter-site variability using a single peat core from the Etang de la Gruyere (EGR) and a signal core from the Tourbiere de Genevez (TEG) bogs, located 3.5 km from one another in Switzerland. The intra-site variability in absolute values of Hg AR exceeded the intra-core variability during the pre-industrial period between EGR, 1.0 ± 0.3 µg $m^{-2}y^{-1}$ (25% RSD), and TEG, 1.6 ± 0.4 µg $m^{-2}y^{-1}$ (30% RSD). During the industrial period (after 1700 AD) both the maximum and average Hg AR were also higher at TEG, 12.6 ± 7.7 µg $m^{-2}y^{-1}$ (61% RSD) than at EGR, 17.0 ± 13.1 µg $m^{-2}y^{-1}$ (77% RSD). However, relative increase factors were very similar between the two sites when comparing pre-Industrial to maximum (30× vs. 28×) and average Industrial period Hg accumulation (12× vs. 11×). Based on this we conclude that bog-specific characteristics prevent the comparison of absolute Hg deposition rates between bogs, but that relative increase factors obtained from different bogs are valid indicators of changes in Hg deposition.

The objective of the multi-coring approach taken in this study was to investigate the intra-site variability in Hg AR reconstructions on a scale of 10 to 100 m. Fig. 6 compares the Hg AR in the four cores. First, the Hg AR profiles agree fairly well between the four cores ($r \geq 0.87$, Table 4). The broad 20th century maximum Hg AR occurs in pollen zones 5 and 6 in all cores and at different locations with respect to the acrotelm–catotelm boundary. Intra-core and intra-site variability is summarized in Table 4. Pre-Industrial Hg AR from the 5th to the 14th century averaged 1.8 ± 0.5 µg $m^{-2}y^{-1}$ (27% RSD). Maximum Hg AR between the 1930s and the 1990s averaged 105 ± 37 µg $m^{-2}y^{-1}$ (36% RSD). Post-1990 declines in Hg AR stabilized around 23 ± 10 µg $m^{-2}y^{-1}$ (41% RSD). However, the core M2 maximum Hg AR of 53 ± 33 µg $m^{-2}y^{-1}$ and the core M1 pre-Industrial Hg AR of 2.4 ± 1.5 µg $m^{-2}y^{-1}$ were significantly different from the other cores ($p < 0.02$). This shows that reconstructions of Hg AR that are based on a single peat core have a high statistical chance of showing core-specific values that are not representative of the bog as a whole (Bindler et al., 2004; Martinez Cortizas et al., 2012). Taking the core M2, Hg AR maximum of 53 µg $m^{-2}y^{-1}$ as an example, a single core study may deviate from the bog average (105 µg $m^{-2}y^{-1}$) by as much as 100%. Despite these significant differences, the outlier observations on cores M2 and M1 do not exceed a variation of 2SD around the mean and were therefore retained in calculating the bog averaged Hg AR trends. The multi-coring approach taken in this study results in overall uncertainties associated with pre-Industrial, maximum 20th century, and post-maximum reconstructed Hg AR that are similar and around 30 to 40% RSD.

Potential factors that could contribute to this intra-site variation are micro-climatic variations affecting Hg deposition and soil re-emission,

Table 4
Summary and intra-site comparison of reconstructed mercury accumulation rates (Hg AR, μg m^{-2} y^{-1}) for the four Misten cores.

Core ID	Pre-Industrial	Maximum	Post-maximum	Max./pre-Ind.	Max./post-max.
01W	2.4 ± 1.5 (62%)	126 ± 31 (25%)	20 ± 7 (37%)	53	6.4
04W	1.7 ± 1.5 (89%)	53 ± 33 (62%)	18 ± 11 (60%)	32	3.0
05W	1.3 ± 0.5 (38%)	137 ± 49 (36%)	37 ± 22 (60%)	107	3.7
06W	1.7 ± 0.6 (34%)	103 ± 17 (17%)	8.3 ± 0.6 (7%)	60	12
Average	1.8 ± 0.5 (27%)	105 ± 37 (36%)	21 ± 12 (58%)	63 ± 31 (50%)	6.4 ± 4.3 (68%)

micro-topography and lateral run-off, or canopy effects when trees are present (Roos-Barraclarough et al., 2003; Biester et al., 2007). The average relative increase factors between pre-Industrial and maximum Hg AR, 63 ± 31 (% RSD) and average anthropogenic period Hg AR and maximum Hg AR, 4.8 ± 1.7 (% RSD) for the Misten cores. The variations in relative increase factors between the four Misten cores are much larger than for the cited Swiss the Etang de la Gruyere (EGR) and the Tourbiere de Genevez (TEG) bogs, which may be related to the overall inhomogeneous peat accumulation rates across time and space at Misten.

4.3. Comparison of the Misten bog with others sites

Hg accumulation rates reconstructed from the Misten peat cores are comparable to results obtained from other European bogs. The mean pre-Industrial Hg accumulation rate (before 1300 AD, 1.8 ± 0.5 μg $m^{-2}y^{-1}$, 1SD) for M1, M2, M3 and M4 is similar to published values of 0.3–8 μg $m^{-2}y^{-1}$ from 12,500 BC to1300 AD for a Swiss peat bog (Roos-Barraclough et al., 2003), 0.3–3 μg $m^{-2}y^{-1}$ obtained from 200 AD to 950 AD for a Greenland peat bog (Shotyk et al., 2003) , and 1.4 ± 1 μg $m^{-2}y^{-1}$ from 5700 BC to 1470 AD for 3 sites in Southern Ontario, Canada (Givelet et al., 2004a, 2004b). Those studies suggested that Hg accumulation rates in several ombrotrophic bogs, during pre-Industrial period correspond mainly to natural Hg deposition.

During the Industrial revolution, the maximum Hg accumulation rates in the Misten peat bogs were within the range 90 to 190 μg $m^{-2}y^{-1}$ (1930–1990 AD). This is in good agreement with the maximum values recorded in peat bogs in Switzerland (79 to 108 μg $m^{-2}y^{-1}$) from 1911 AD to 1973 AD (Roos-Barraclough et al., 2002), Greenland and Denmark (164–184 μg $m^{-2}y^{-1}$, Shotyk et al., 2003) in 1953 AD, Ontario peat bogs in Canada (55–141 μg $m^{-2}y^{-1}$) from 1950 to 1960 AD (Givelet et al., 2004a, 2004b), and Flanders Moss in Scotland 77–183 μg $m^{-2}y^{-1}$ from 1923 to 1948 AD (Farmer et al., 2009). In the Misten cores, the recent Hg accumulation rate from 1990 to 2008 AD (23 ± 10 μg $m^{-2}y^{-1}$) is similar to the 35 ± 5 μg $m^{-2}y^{-1}$ in Switzerland (Roos-Barraclough et al., 2002) and 27 ± 15 μg $m^{-2}y^{-1}$ for 4 Scottish cores (Farmer et al., 2009) but 2 times lower that what observed in recent peat layers of Czech Republic (Zuna et al., 2012).

4.4. Anthropogenic Hg sources to the Misten bog

The records of Hg accumulation rates found in the Misten bog are in good agreement with the history of the global production of Hg over the past 500 years reported by Hylander and Meili (2003) and of European coal production over the past 200 years (Rutledge, 2011) (Fig. 7). Mercury shows that Hg accumulation rates increase in cores M1 and M4 in parallel with the global production of Hg from 1500 to 1800 AD. Based on the data from these cores, during this period Hg accumulation rates increased from 2 to 28 μg $m^{-2}y^{-1}$ in M1 and from 1 to 3 μg $m^{-2}y^{-1}$ in core M4. This increase in Hg accumulation rate can be explained by Hg mining and metallurgy emissions in Almadén (Spain) and Idrija in Slovenia (Hylander and Meili, 2003). The total Hg production from 1500 to 1800 AD in these mines was 150,000 tons (17% from the global production in the last 500 years, Hylander and Meili, 2003). Between 1800 and 1850 AD, the global production of Hg decreased from 57,000 to 49,000 tons (Hylander and Meili, 2003), but the total Hg accumulation rates in Misten cores continued to increase (Fig. 7). This increase coincided with a maximum of European production of Hg (47,000 tons, 5% from the global Hg production) and a maximum Zn–Pb mining activity in Belgium (Dejonghe, 1998; Hylander and Meili, 2003). Average Zn ores contain ~10 mg kg^{-1} of Hg (Hylander and Herbert, 2008). Coal production and industrial use became important in Europe (1.3 million metric tons per year) in 1817 AD and in 1830 AD (2.3 million metric tons per year) in Belgium (Rutledge, 2011). Therefore, Zn–Pb mining and coal burning may have been dominant source of Hg deposition between 1800 and 1850 AD. The increased Hg accumulation rates in the Misten peat cores between 1850 and 1915 AD can be explained by increased European coal production and use, and metal smelting and refinery (Pb and Zn) in Belgium. The European coal production increased up to 400 million metric tons per year in 1913 AD while that in Belgium was up to 25 million metric tons per year between 1900 and 1910 (Fig. 7). The smelter and refinery production (Pb and Zn) in Belgium increased by factor > 100 from 1850 to 1913 (Fig. 7).

In the cores M1 and M4, the maximum Hg accumulation rates between AD 1930 and 1980 are good agreement with the maximum Belgian coal and smelter production (Fig. 7). Coal combustion, non-ferrous mining and refining were the dominant anthropogenic Hg sources from 1930 to 1970 (Shotyk et al., 2003, 2005). Mining activity decreased in Belgium after 1945 (Dejonghe, 1998; Schmitz, 1979). However, the import of Zn–Pb ores from worldwide locations to Belgium has always been larger than local production and fueled the metallurgical industries (Schmitz, 1979; Sonke et al., 2002). Smelter and refinery production of imported (Pb, Cu, and Zn) reached a maximum in 1976 (Fig. 7). This may explain the higher Hg accumulation rate in Misten peat cores (at 19 cm for M1 and at 12 cm for M4). The maximum Pb concentration in core M1 corresponds to the maximum Hg concentration, suggesting a common source of these elements. In the 20th century, coal combustion was the dominant anthropogenic source of both Hg (Lindberg et al., 1987; Shotyk and Krachler, 2010) and Pb (Shotyk et al., 2003, 2005) and is the most likely source for these two elements.

The reduction in Hg accumulation rates in the upper section of the peat cores between 1980 and 2008 follows the same trend as global and the European Hg/coal production. The decline of Hg AR after the 1980s may be linked to the introduction of Hg retaining filters in industrial process and the decline in coal consumption (Fig. 7). The main sources of Hg emissions in Belgium from 1980 to 2008 were chlorine plants, cement production, construction industry and mining and various industrial emissions (Mukherjee et al., 2004, 2008).

According to Ilyin et al. (2010), the atmospheric Hg deposition measured at 8 Belgian sites, from 1990 to 2008, demonstrate a declining trend. In 1991 (1987–1994 AD), the Hg accumulation rate was 67 μg $m^{-2}y^{-1}$ over Belgium, close to that in cores M1 and M4. By 2009, atmospheric Hg deposition reduced to 19 μg $m^{-2}y^{-1}$ (Ilyin et al., 2010), which again is in good agreement with reconstructed Hg AR at Misten of 18 μg $m^{-2}y^{-1}$ in the surface peat layers (2007–2008 AD) and modeled data by EMEP (Ilyin et al., 2010, 2011; Travnikov et al., 2012). The modeled trend of Hg

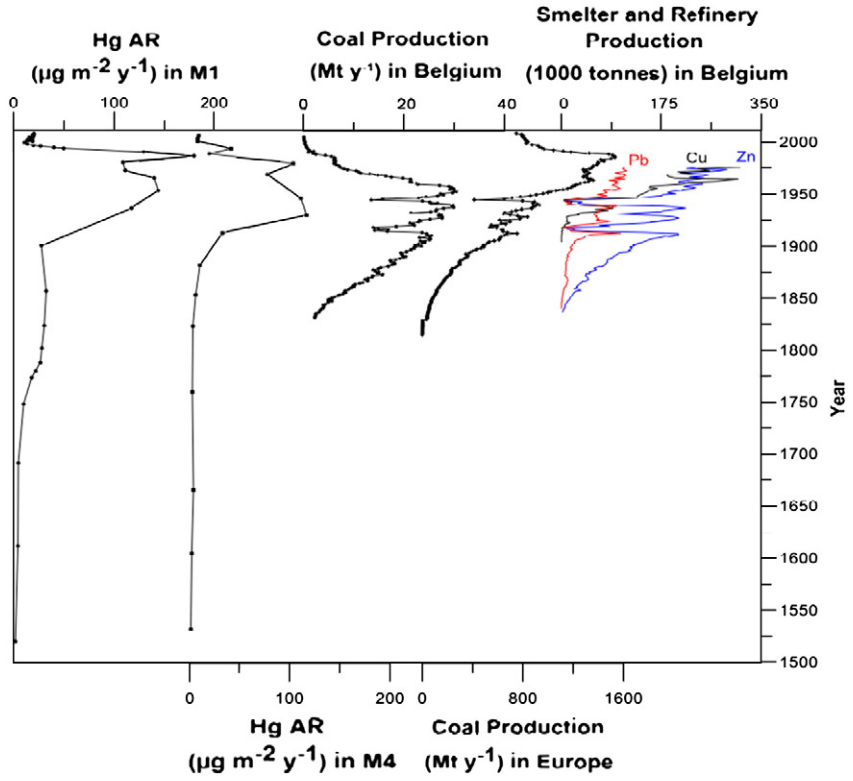

Fig. 7. Comparison between total accumulation rates in M1 and M4 cores with the Belgium and European production of coal (Rutledge, 2011), and with smelter and refinery production (Pb, Cu and Zn) in Belgium (Rutledge, 2011).

deposition over Belgium (Travnikov et al., 2012) is in good agreement with the estimation of Hg AR by Misten peat cores over the period 1990–2008.

5. Conclusions

The four Misten peat cores recorded the historical evolution of Hg accumulation rates over the last 1500 years. The comparison between the pollen zones in the four cores of the Misten peat bogs and the ^{210}Pb–^{14}C dating in the cores M1 and M4 shows that the Misten peat accumulation is rather heterogeneous. There is a good agreement between the AR chronologies of the four Misten peat cores, as assessed independently by ^{14}C–^{210}Pb combined chronologies and pollen timing zones. Our results show that despite different peat accumulation rates in the four cores, the Hg peaks in each core are always located in layers with the same age.

The multiproxy approach measured in core M1 (Fe/Mn ratio, and Pb profile) and the humification calculated for all cores show that Hg is not influenced by redox processes and is an immobile element in Misten peat bog.

At the Misten bog, pre-Industrial Hg accumulation rate averaged 1.8 ± 0.5 µg $m^{-2}y^{-1}$ between 500 AD to 1300 AD. The highest Hg accumulation rates were observed during the 20th century (105 ± 37 µg $m^{-2}y^{-1}$). The maximum Hg accumulation rates ranging from 90 to 200 µg $m^{-2}y^{-1}$ are recorded between 1930 and 1980 AD. The Hg accumulation rate in the Industrial period seems to have been primarily caused by the regional domestic and industrial coal use and smelter and refinery activity (Pb, Cu, and Zn). This study shows the necessity of multi-coring of peat bogs to avoid biased absolute Hg AR reconstructions due to variations in natural biogeochemical and climatic processes. Estimated trends in Hg accumulation rates by peat cores and measured and modeled atmospheric fluxes measured by EMEP in Belgium were in good agreement for the period 1990–2008 with a decrease of a factor ~3–5 over this period.

Acknowledgments

This study was funded by the Walloon Region and the FNRS. This work is supported by research grants ANR-09-JCJC-0035-01 from the French Agence Nationale de Recherche and ERC-2010-StG_20091028 from the European Research Council. M. Allan receives funding from the government of Syria. Frederic Candaudap and Aurelie Lanzanova are thanked for their assistance with ICPMS analysis at GET. We also acknowledge Anson Mackay from UCL and Mae Sexauer Gustin for their contributions on the final version of the manuscript.

References

Appleby PG. Chronostratigraphic techniques in recent sediments. In: Last WM, Smol JP, editors. Tracking environmental change using lake sediments. Basin analysis, coring, and chronological techniquesKluwer; 2001. p. 171–203.

Appleby PG. Three decades of dating recent sediments by fallout radionuclides: a review. Holocene 2008;18(1):83–93.

Benoit JM, Fitzgerald WF, Damman AWH. The biogeochemistry of an ombrotrophic bog: evaluation of use as an archive of atmospheric mercury deposition. Environ Res 1998;78(2):118–33.

Biester H, Kilian R, Franzen C, Woda C, Mangini A, Schöler HF. Elevated mercury accumulation in a peat bog of the Magellanic Moorlands, Chile (53°S) — an anthropogenic signal from the Southern Hemisphere. Earth Planet Sci Lett 2002;201(3–4):609–20.

Biester H, Martinez-Cortizas A, Birkenstock S, Kilian R. Effect of peat decomposition and mass loss on historic mercury records in peat bogs from Patagonia. Environ Sci Technol 2003;37:32–9.

Biester H, Hermanns YM, Martinez-Cortizas A. The influence of organic matter decay on the distribution of major and trace elements in ombrotrophic mires — a case study from the Harz Mountains. Geochim Cosmochim Acta 2012;84:126–36.

Biester H, Bindler R, Martinez-Cortizas A, Engstrom DR. Modeling the past atmospheric deposition of mercury using natural archives: Environ Sci Technol 2007;41:4851–60.

Bindler R, Brannvall ML, Renberg I. Natural lead concentrations in pristine boreal forest soils and past pollution trends: a reference for critical load models. Environ Sci Technol 1999;33:3362–7.

Bindler R, Renberg I, Anderson NJ, Appleby PG, Emteryd O, Boyle J. Lead isotope ratios of lake sediments in West Greenland: inferences on pollution sources. Atmos Environ 2001;35:4675–85.

Bindler R, Klarqvist M, Klaminder J, Forster J. Does within-bog spatial variability of mercury and lead constrain reconstructions of absolute deposition rates from single peat records? The example of Store Mosse, Sweden. Global Biogeochem Cycles 2004;18:1-11.

Blaauw M, Christen JA. Flexible paleoclimate age-depth models using an autoregressive gamma process. Bayesian Anal 2011;6:457–74.

Bronk Ramsey C. Bayesian analysis of radiocarbon dates. Radiocarbon 2009;51(1): 337–60.

Chambers FM, Booth RK, De Vleeschouwer F, Lamentowicz M, Le Roux G, Mauquoy D, Nichols JE, van Geel B. Development and refinement of proxy-climate indicators from peats. Quat Int 2011;268:21–33.

Cloy JM, Farmer JG, Graham MC, MacKenzie AB, Cook GT. Historical records of atmospheric Pb deposition in four Scottish ombrotrophic peat bogs: an isotopic comparison with other records from western Europe and Greenland. Global Biogeochem Cycles 2008;22:GB2061.

Coggins AM, Jennings SG, Ebinghaus R. Accumulation rates of the heavy metals lead, mercury and cadmium in ombrotrophic peatlands in the west of Ireland. Atmos. Environ. 2006;40:260–78.

De Vleeschouwer F, Gérard L, Goormaghtigh C, Mattielli N, Le Roux G, Fagel N. Atmospheric lead and heavy metal pollution records from a Belgian peat bog spanning the last two millennia: human impact on a regional to global scale. Sci Total Environ 2007;377(2–3):282–95.

De Vleeschouwer F, Sikorski J, Fagel N. Development of lead 210 measurement in peat using polonium extraction. A comparison of techniques. Geochronometria 2010;36: 1–8.

De Vleeschouwer F, Pazdur A, Luthers C, Streel M, Mauquoy D, Wastiaux C, et al. A millennial record of environment change in peat deposits from the Misten (East Belgium). Quat Int 2012;268:44–57.

Dejonghe L. Zinc–lead deposits of Belgium. Ore Geol Rev 1998;12(5):329–54.

Farmer JG, Anderson P, Cloy JM, Graham MC, MacKenzie AB, Cook GT. Historical accumulation rates of mercury in four Scottish ombrotrophic peat bogs over the past 2000 years. Sci Total Environ 2009;407(21):5578–88.

Fitzgerald WF, Lamborg CH. Geochemistry of mercury in the environment. In: Heinrich DH, Karl KT, editors. Treatise on geochemistry. Oxford: Pergamon; 2007. p. 1-47.

Givelet N, Roos-Barracl F, Shotyk W. Atmospheric mercury accumulation rates between 5900 and 800 calibrated years BP in the high Arctic of Canada recorded by Peat Hummocks. Environ Sci Technol 2004a;38(0013-936X):4964–72.

Givelet N, Le Roux G, Cheburkin A, Chen B, Frank J, Goodsite ME, et al. Suggested protocol for collecting, handling and preparing peat cores and peat samples for physical, chemical, mineralogical and isotopic analyses. J Environ Monit 2004b;6:481–92.

Gobeil C, Macdonald RW, Smith JN. Mercury profiles in sediments of the Arctic Ocean basins. Environ Sci Technol 1999;33:4194–8.

Hylander LD, Herbert RB. Global emission and production of mercury during the pyrometallurgical extraction of nonferrous sulfide ores. Environ Sci Technol 2008;42(16):5971–7.

Hylander LD, Meili M. 500 years of mercury production: global annual inventory by region until 2000 and associated emissions. Sci Total Environ 2003;304(1–3):13–27.

Ilyin I, Rozovskaya O, Sokovykh V, Travnikov O, Varygina M. Heavy metals: transboundary pollution of the environment. EMEP status report 2/2010. MSC-E; 2010 [107 pp.].

Ilyin I, Rozovskaya O, Travnikov O, Varygina M. Heavy metals: transboundary pollution of the environment. EMEP status report 2/2011 June; 2011 [92 pp.].

Jensen A, Jensen A. Historical deposition rates of mercury in Scandinavia estimated by dating and measurement of mercury in cores of peat bogs. Water Air Soil Pollut 1990;56:769–77.

Klaminder J, Renberg I, Bindler R, Emteryd O. Isotopic trends and background fluxes of atmospheric lead in Northern Europe: analyses of three ombrotrophic bogs from south Sweden. Global Biogeochem Cycles 2003;17. [Art. No. 1019].

Krachler M, Mohl C, Emons H, Shotyk W. Influence of digestion procedures on the determination of rare earth elements in peat and plant samples by USN–ICP-MS. J Anal At Spectrom 2002;17:844–51.

Le Roux G, Aubert D, Stille P, Krachler M, Kober B, Cheburkin A, et al. Recent atmospheric Pb deposition at a rural site in southern Germany assessed using a peat core and snowpack, and comparison with other archives. Atmos Environ 2005;39(36):6790–801.

Lindberg S, Bullock R, Ebinghaus R, Engstrom D, Feng X, Fitzgerald W, Pirrone N, Prestbo E, Seigneur Ch. Asynthesis of progress and uncertainties in attributing the sources of mercury in deposition. Ambio 2007;36:19–32.

Lindberg SE, Stockes PM, Goldberg E, Wren C. In: Hutchinson TC, Meem KM, editors. Lead, mercury, cadmium, and arsenic in the environment; 1987. p. 17–33. New York.

Madson P. Peat bog records of atmospheric mercury deposition. Nature 1981;293: 127–30.

Manneville OVV, Villepoux O, Blanchard F, Bremer K, Dupieux N, Feldmeyer-Christe E, et al. Le monde des tourbières et des marais. France, Suisse, Belgique et Luxembourg. Lausanne; 2006.

Martinez Cortizas A, Potevedra-Pombal X, Novoa-Munos JC, Garcia-Rodeja E. Four thousand years of atmospheric Pb, Cd and Zn deposition recorded by the ombotrophic peat bog of Penido Vello. Water Air Soil Pollut 1997;100:387–403.

Martinez Cortizas A, Pontevedra-Pombal X, Garcia-Rodeja E, Novoa-Munoz JC, Shotyk W. Mercury in a Spanish peat bog: archive of climate change and atmospheric metal deposition. Science 1999;284:939–42.

Martinez Cortizas A, Peiteado Varela A, Bindler R, Biester H, Cheburkin A. Reconstructing historical Pb and Hg pollution in NW Spain using multiple cores from the Chao de Lamoso bog (Xistral Mountains). Geochim Cosmochim Acta 2012;82:68–78.

Matty JM, Long DT. Early diagenesis of mercury in the Laurentian Great Lakes. J Great Lakes Res 1995;21(4):574–86.

Mergler D, Anderson HA, Hing Man Chan L, Mahaffey KR, Murray M, Sakamoto M, et al. Methylmercury exposure and health effects in humans: a worldwide concern. Ambio 2007;36:3-11.

Morel FMM, Kraepiel AML, Amyo M. The chemical cycle and bioaccumulation of mercury. Annu Rev Ecol Syst 1998;29:543–66.

Mukherjee AB, Zevenhoven R, Brodersen J, Hylander LD, Bhattacharya P. Mercury in waste in the European Union: sources, disposal methods and risks. Resour Conserv Recycl 2004;42(2):155–82.

Mukherjee AB, Zevenhoven R, Bhattacharya P, Sajwan KS, Kikuchi R. Mercury flow via coal and coal utilization by-products: a global perspective. Resour Conserv Recycl 2008;52(4):571–91.

Norton SA, Evans GC, Kahl JS. Comparison of Hg and Pb fluxes to hummocks and hollows of ombrotrophic Big Heath bog and to nearby Sargent Mt. Pond, Maine, USA. Water Air Soil Pollut 1997;100:271–86.

Novák M, Emmanuel S, Vile MA, Erel Y, Véron A, Paes T, et al. Origin of lead in eight central European peat bogs determined from isotope ratios, strengths, and operation times of regional pollution sources. Environ Sci Technol 2003;37:437–45.

Outridge PM, Rausch N, Percival JB, Shotyk W, McNeely R. Comparison of mercury and zinc profiles in peat and lake sediment archives with historical changes in emissions from the Flin Flon metal smelter, Manitoba, Canada. Sci Total Environ 2011;409:548–63.

Pacyna EG, Pacyna JM, Steenhuisen F, Wilson S. Global anthropogenic mercury emission inventory for 2000. Atmos Environ 2006;40(22):4048–63.

Piotrowska N, Vleeschouwer FD, Sikorski J, Pawlyta J, Fagel N, Le Roux G, et al. Intercomparison of radiocarbon bomb pulse and 210Pb age models. A study in a peat bog core from North Poland. Nucl Instrum Methods Phys Res, Sect B 2010;268(7–8):1163–6.

Piotrowska N, Blaauw M, Mauquoy D, Chambers, FM. Constructing deposition chronologies for peat deposits using radiocarbon dating. Mires Peat 2011;7:1-14. [Article 10].

Pirrone N, Keating T. Hemispheric transport of air pollution. Air pollution studies no. 18. Part B: mercury978-92-1-117044-3; 2010.

Pirrone N, Mason R. Mercury fate and transport in the global atmosphere: emissions, measurements and models. USA: Springer978-0-387-93957-5; 2009. p. 637.

Quinty F, Rochefort L. Peatland restoration guide. 2nd ed. Québec, Québec: Canadian Sphagnum Peat Moss Association et New Brunswick Department of Natural Resources and Energy; 2003 [106 pp.].

Reimer PJ, Baillie MGL, Bard E, Bayliss A, Beck JW, Blackwell PG, Bronk Ramsey C, et al. IntCal09 and Marine09 radiocarbon age calibration curves, 0-50,000 years cal BP. Radiocarbon 2009;51(4):1111–50.

Roos-Barraclough F, Shotyk W. Millennial-scale records of atmospheric mercury deposition obtained from ombrotrophic and minerotrophic peat from the Swiss Jura Mountains. Environ Sci Technol 2003;37(2):235–44.

Roos-Barraclough F, Martinez-Cortizas A, Garcla-Rodeja E, Shotyk W. A 14500 year record of the accumulation of atmospheric mercury in peat: volcanic signals, anthropogenic influences and a correlation to bromine accumulation. Earth Planet Sci Lett 2002;202(2):435–51.

Rutledge D. Estimating long-term world coal production with logit and probit transforms. Int J Coal Geol 2011;85:23–33.

Rydberg J, Karlsson J, Nyman R, Wanhatalo I, Näthe K, Bindler R. Importance of vegetation type for mercury sequestration in the northern Swedish mire, Rödmossamyran. Geochim Cosmochim Acta 2010;74(24):7116–26.

Schmitz CJ. World non-ferrous metal production and prices, 1700–1976. London: Frank Cass and Co; 1979.

Schroeder WH, Munthe J. Atmospheric mercury—an overview. Atmos Environ 1998;32(5):809–22.

Shotyk W, Krachler M. The isotopic evolution of atmospheric Pb in central Ontario since AD 1800, and its impacts on the soils, waters, and sediments of a forested watershed, Kawagama Lake. Geochim Cosmochim Acta 2010;74(7):1963–81.

Shotyk W, Cheburkin K, Appleby PG, Fankhauser A, Kramers JD. Two thousand years of atmospheric arsenic, antimony, and lead deposition recorded in an ombrotrophic peat bog profile, Jura Mountains, Switzerland. Earth Planet Sci Lett 1996;145(1–4):E1–7.

Shotyk W, Weiss D, Appleby PG, Cheburkin AK, Frei R, Gloor M, et al. History of atmospheric lead deposition since 12,370 ^{14}C yr BP recorded in a peat bog profile, Jura Mountains, Switzerland. Science 1998;281:1635–40.

Shotyk W, Weiss D, Kramers JD, Frei R, Cheburkin AK, Gloor M, Reese S. Geochemistry of the peat bog at Etang de la Gruère, Jura Mountains, Switzerland, and its record of atmospheric Pb and lithogenic trace metals (Sc, Ti, Y, Zr, and REE) since 12370 14C yr BP. Geochim Cosmochim Acta 2001;65(14):2337–60.

Shotyk W, Goodsite ME, Roos-Barraclough F, Frei R, Heinemeier J, Asmund G, et al. Anthropogenic contributions to atmospheric Hg, Pb and As accumulation recorded by peat cores from southern Greenland and Denmark dated using the ^{14}C "bomb pulse curve". Geochim Cosmochim Acta 2003;67(21):3991–4011.

Shotyk W, Goodsite ME, Roos-Barraclough F, Givelet N, Le Roux G, Weiss D, et al. Accumulation rates and predominant atmospheric sources of natural and anthropogenic Hg and Pb on the Faroe Islands. Geochim Cosmochim Acta 2005;69(1): 1-17.

Sikorski J, Bluszcz A. Application of α and γ spectrometry in the ^{210}Pb method to model sedimentation in artificial retention reservoir. Geochronometria 2008;31:65–75.

Sonke JE, Hoogewerf JA, van der Laan SR, Vangronsveld JA. Chemical and mineralogical reconstruction of Zn-smelter emissions in the Kempen region (Belgium), based on organic pool sediment cores. Sci Total Environ 2002;292:101–19.
Steinmann P, Shotyk W. Chemical composition, pH, and redox state of sulfur and iron in complete vertical porewater profiles from two Sphagnum peat bogs, Jura Mountains, Switzerland. Geochim Cosmochim Acta 1997;61(6):1143–63.
Travnikov O, Ilyin I, Rozovskaya O, Varygina M. Long-term changes of heavy metal transboundary pollution of the Environment (1990–2010). EMEP status report 2/2012 June; 2012 [63 pp.].
Vincens A, Le'zine A, Buchet G, Lewden D, Le Thomas A. African pollen database inventory of tree and shrub pollen types. Rev Palaeobot Palyno 2007;145:135-14.
Wastiaux C, Schumacker R. Topographie de surface et de subsurface des zones tourbeuses des réserves naturelles domaniales des Hautes-Fagnes. Convention C60 entre le Ministère de la Région Wallonne, Direction générale des Ressources naturelles et de l'Environnement, et l'Université de Liège. Unpublished report 2003. 52 p. +annexes. [In French].
Wilson SJ, Steenhuisen F, Pacyna JM, Pacyna EG. Mapping the spatial distribution of global anthropogenic mercury atmospheric emission inventories. Atmos Environ 2006;40(24):4621–32.
Zaccone C, Santoro A, Cocozza C, Terzano R, Shotyk W, Miano TM. Comparison of Hg concentrations in ombrotrophic peat and corresponding humic acids, and implications for the use of bogs as archives of atmospheric Hg deposition. Geoderma 2009;148(3–4):399–404.
Zuna M, Ettler V, Šebek O, Mihaljevič M. Mercury accumulation in peatbogs at Czech sites with contrasting pollution histories. Sci Total Environ 2012;424:322–30.